Modern Chemistry & Applications
ISSN: 2329-6798

Solá, Mod Chem appl 2014, 2:1
DOI: 10.4172/2329-6798.1000116

Research Article Open Access

Electrical Properties of Pristine and Electron Irradiated Carbon Nanotube Yarns at Small Length Scales

Francisco Solá*
NASA Glenn Research Center, Materials and Structures Division, Cleveland, OH 44135, USA

Abstract

In this report the effect of e-beam irradiation on Carbon Nanotube (CNT) yarns electrical resistivity was studied by employing electron beam irradiation on a Transmission Electron Microscope (TEM) follow by two probe resistivity method in a Scanning Electron Microscope (SEM). Both local crosslinking and amorphous regions within the CNT yarn were observed with increased electron dosage, as revealed by High Resolution TEM (HRTEM). The resistivity lower bound value was obtained at the maximum dosage used, which was below the resistivity of the pristine yarn. The resistivity data is explained by a proposed model that takes into account the microstructural changes.

Keywords: CNTs; Crosslinking; Defects; E-beam irradiation; Electrical resistivity; FIB; SEM; TEM

Introduction

NASA is currently exploring routes to potentially replace conventional carbon fiber composites with CNT based composite materials. This could translate to approximately a one-third reduction of unfueled weight of space vehicles and structures, and if successful, will diminish considerably vehicle launch costs. To achieve this, commercially available CNT based materials must have at least two times the strength of conventional carbon fibers. CNT yarns are currently one of the best commercially available CNT based materials in terms of mechanical properties. However, their tensile strength is about half of conventional carbon fibers. This is related to the weak shear interactions between carbon shells and bundles within a yarn [1]. Therefore, current efforts are focused in developing protocols to improve the mechanical properties of these materials.

One potential route to achieve the mechanical improvement is the cross-linking method induced by electron beam irradiation. The weak shear interactions between adjacent C-shells/CNT can be improved by the formation of sp^3 C-C bonds induced by e-beam irradiation [1]. This can occur at both the interwall sites of individual multiwall CNT (MWCNT) and between CNTs neighbors and both can potentially increase the mechanical response of CNT yarns [2,3]. E-beam energies greater than 80 keV are needed to displace C atoms and to induce complex kinetics and recombination of lattice defects within the hexagonal carbon network, which eventually leads to cross-linking [4]. For one isolated MWCNT (and small bundles), 100-200 keV are effective energies to crosslink [5,6]. Being CNT yarns fibers composed of several MWCNTs, the question arises as to what extend energies in this range will still promote crosslinking effectively.

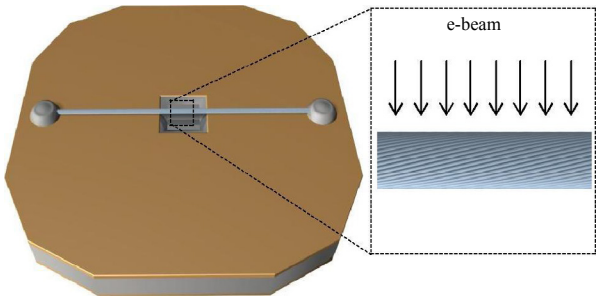

Figure 1: Schematic of the sample mount for e-beam irradiation in the TEM. Gray and gold color corresponds to silicon and silicon nitride materials, respectively. Note that only the segment of the CNT yarn that lies in the hole of the TEM sample mount is exposed to e-beam irradiation.

The study of the electrical response of CNT yarns as a function of electron dose can be a complementary route to monitor possible cross-linking events, and is important to establish multifunctional properties of CNT yarns. Potential applications of CNT yarns that possess both good electrical and mechanical properties include antennas and lightning strike protection of aircraft [7]. Considerable efforts have been focused until now in e-beam irradiation methods that lead to mechanical improvement. Although Mikó and coworkers reported the effects of e-beam irradiation on the electrical resistivity of Single-Walled CNT (SWCNT) fiber systems [8,9], work on the e-beam irradiation effects on the electrical properties of CNT yarns is lacking. In this brief report, small segments of CNT yarns are exposed to e-beam irradiation in a TEM operated at 200 keV and at different doses. The electrical resistivity as a function of e-beam irradiation is studied by the two probe method, using micromanipulators inside an SEM.

Experimental

CNT yarns were obtained from Nanocomp Technologies, Inc. As-received samples from Batch 5279 were used in this work. E-beam irradiation experiments were performed in a TEM Philips CM200 microscope [10] operated with a beam energy of 200 keV, and e-beam flux of ~ 5×10^{12} e/cm^{2}s.

Small segments of CNT yarns were mounted on special TEM sample mounts from Norcada, Inc. These TEM windows consist of 5 mm × 5 mm, 200 μm Si frames, decorated from both sides with a silicon nitride film of ~100 nm. The silicon nitride films serve as electrical isolation material. In the center of the TEM sample mount there is an open (without silicon nitride material) 0.5 mm×0.5 mm area that provides a compatible window for both e-beam irradiation experiments and TEM imaging investigation. A schematic of the e-beam irradiation is depicted in Figure 1. Possible microstructural changes on the CNT yarns were monitored by high resolution HRTEM using a Gatan Imaging Filter (GIF) camera.

***Corresponding author:** Francisco Solá, NASA Glenn Research Center, Materials and Structures Division, Cleveland, OH 44135, USA, Tel: +1-216-433-6954; Fax: +1-216-977-7132; E-mail: francisco.sola-lopez@nasa.gov

Received December 25, 2013; **Accepted** January 20, 2014; **Published** January 23, 2014

Citation: Solá F (2014) Electrical Properties of Pristine and Electron Irradiated Carbon Nanotube Yarns at Small Length Scales. Mod Chem appl 2: 116. doi:10.4172/2329-6798.1000116

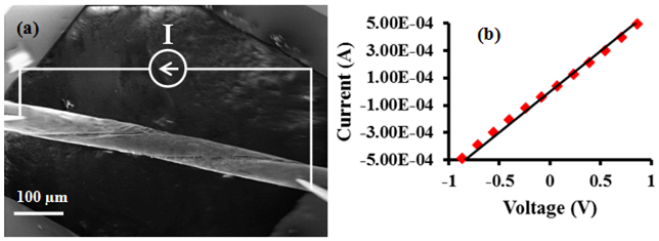

Figure 2: (a) SEM image of 2 tungsten probe electrical set-up measurement. Note that data collection was done under current source mode. (b) Example of current versus voltage graph used to estimate the resistivity. The red dots are experimental data and the black line is an Ohms law fit.

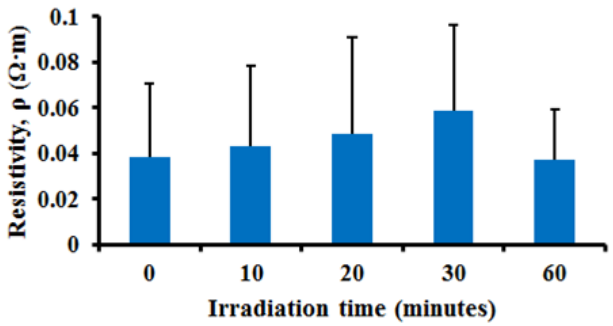

Figure 3: Effect of e-beam irradiation on CNT yarn resistivity. Four samples were tested for each case.

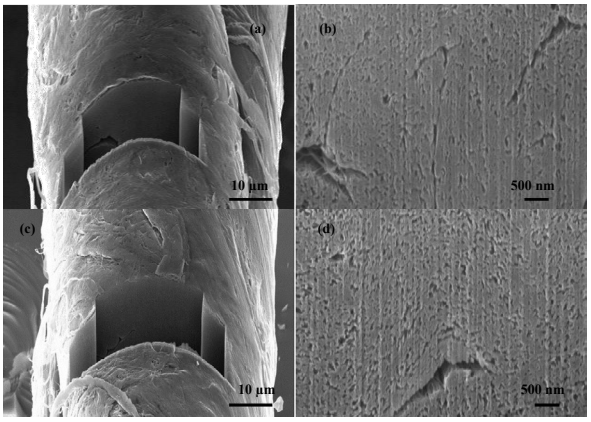

Figure 4: FIB/SEM cross section analysis of the same pristine CNT yarn at different length locations,(a) and (c) low magnification images,(b) and (d) high magnification images.

Resistivity studies were done inside (in vacuum) an Auriga Focused Ion Beam (FIB) microscope from Carl Zeiss, with a specimen vacuum of ~ 10^{-6}Torr [11]. The Auriga instrument is a crossbeam FIB instrument, but only the electron beam column was used for image formation, which means that it was used as a standard SEM. All SEM images were acquired using an In-lens Secondary Electron (SE) detector [12,13], and a beam energy of 5 keV. Two electrochemically etched tungsten tips were connected to two Kleindiek micromanipulators equipped with low current plug-ins [14]. Electrical experiments were controlled with a Keithley 2400 source meter in current source mode, and a LabView program. The SEM beam was blanked before collecting the data. The vacuum chamber, including the micromanipulators and sample stage holder, were cleaned with a plasma cleaner to remove contamination, prior to sample insertion. The sample itself and the TEM sample mounts were not exposed to plasma cleaning, as this creates defects on the yarns and damage the silicon nitride films.

Cross section imaging of the CNT yarns was conducted in the Auriga microscope. Milling procedures involved the formation of a trench in the CNT yarns using an ion beam current of 2nA at 30 kV, followed by low current cleaning steps of the imaged surface [15].

Results and Discussion

Figure 1 depicts the schematic of the sample mount for e-beam irradiation in the TEM. Only the segment of the CNT yarn that lies in the hole of the TEM sample mount is exposed to e-beam irradiation. Figure 2a is a SEM image which illustrates the two probe electrical characterization of CNT yarns. Typically, the measurements were conducted to probe CNT yarns length of ~ 450 µm, and diameters of ~ 77-84 µm. An example of current versus voltage dependence is plotted in Figure 2b. Note that the relationship is linear and therefore the use of Ohm's law (V = IR) to estimate system resistance (R) is justified. To estimate the resistivity of CNT yarns, the experimental set-up is modeled by a series resistor, where each component resistor is additive, $R_{total} = R_{yarn} + \Sigma R_{other}$ (internal electrical source resistance, cables and W probes). Furthermore, contact resistance is assumed to be negligible here. This is a reasonable assumption when a considerably pressure force between probe and sample is established [16], as in this work. Before establishing contact with the CNT yarns, the two end-tips of the tungsten probes were contacted and conditioned for electrical measurements [17]. By doing so, contact resistance is further reduced, and from the linear current voltage dependence of the conditioned probes, ΣR_{other} can be estimated and extracted from the total resistance to obtain R_{yarn}. Then, the yarns resistivity (ρ) is obtained using equation 1

$$\rho = \pi R_{yarn}^2 \frac{D^2}{4L} \quad (1)$$

where D and L are the diameter and length of the yarn tested, respectively [18], and both quantities can be extracted directly from SEM images.

The electrical resistivity as a function of e-beam irradiation is presented in Figure 3. Irradiation times range from 10-60 min, which correspond to dosages of ~$3x10^{15}$-$2x10^{16}$ e/cm^2. The average values of the resistivity increased with irradiation time for up to 30 min and decrease with further irradiation, though with the presence of scattering in the data. The scattering of the data is attributed to the local variation of the microstructure (diameter, internal porosity as supported in the SEM and focused ion beam microscopy results) of the CNT yarns in Figure 4. Similar local changes in resistivity for larger length scale CNT yarns due to variations in microstructure have been reported [19]. Note that the maximum resistivity at 30 min of irradiation corresponds to an increase of ~ 1.5 times the resistivity of the pristine yarn, and that the resistivity at 60 min is just a slight decrease of the pristine resistivity. For comparison purposes, the resistivity of CNT yarns of the current study are about 10^2 times smaller than aerosol-like (non-twisted) yarns, but are ~10^3 times larger than other twisted yarns (although these values were estimated with yarn segment lengths of 50 mm) [19], and about 10 times higher than SWCNT fibers of 3-5 mm tested length [8,9]. Interestingly, our group at NASA likewise noticed that larger scale CNT yarns irradiated with MeV energies also present scattering of data in regards to tensile strength, something that can be explained also by local variations on the yarn microstructure [20]. The results were that the maximum tensile strength of the yarns was obtained at the maximum e-beam irradiation dosage.

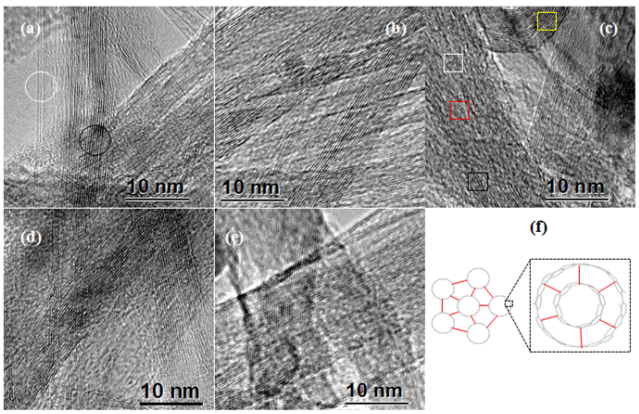

Figure 5: HRTEM of CNT yarns of pristine (a), e-beam irradiated at10 min (b), 20 min (c), 30 min (d), and 60 min (e). Scale bar is 10 nm. (f) Schematic that explains possible cross linking sites of CNT within the yarn, which are at bundle and isolated nanotube sites.

To obtain possible explanations to the e-beam irradiation effects on resistivity, the author conducted HRTEM analysis on the microstructure of CNT yarns. HRTEM of CNT yarns of pristine (a), e-beam irradiated with10 min (b), 20 min (c), 30 min (d), and 60 min (e), are presented in Figure 5. Figure 5f is a schematic that summarizes possible crosslinking sites (marked with red lines) of CNT constituents within the yarn at two different scales. The images were taken in thin areas located at the edges of the yarns. From these images, the different planes of CNTs oriented in a given twisted direction can be observed.

For the purpose of the following discussion, only areas of the images that are in focus are described. The area enclosed by a white circle in Figure 5a shows that the CNTs of yarns are double walled, while the area enclosed by a black circle is consistent with a CNT bundle structure. The alternating black/white fringes correspond to the lattice planes of CNTs in the bundle, with each lattice plane built from a row of CNTs [21,22]. Crosslinking sites on CNTs can be monitored by these HRTEM images and typically correspond to areas where the fringes are less coherent but do not lose completely their structure to form an amorphous carbon (a-C) structure [2]. Cross-linking events can be observed at 10 min of irradiation (Figure 5b). Several types of microstructural changes of CNTs within the yarn are evident at 20 min of irradiation (Figure 5c). These include cross-linked sites (area enclosed by a black box), pristine-non-cross-linked sites (yellow box), a-C structure sites (red box), and sites with a mixture of a-C and cross-linked sites (white box). With further irradiation it can be seen that both a-C and cross-linked sites grow, however, in overall, the crystallinity (fringes structure) of the CNTs is preserved (in the sense that it is not totally lost).

In order to understand these microstructural changes and how to correlate them to the corresponding resistivity results, a brief explanation on e-beam irradiation on CNT defect formation is needed. E-beam electrons can displace C atoms located at the hexagonal lattice network of CNT, only when a critical minimum energy is used known as the displacement threshold. However, the displacement threshold depends on the local arrangement of carbon atoms relative to the electron beam and type of CNT. This is due to the direction of momentum transfer to C atoms distributed in the hexagonal lattice. For instance, displacement threshold energies of 82 keV have been reported for small CNTs oriented perpendicular to the e-beam, and up to 240 keV for relative bulky CNTs oriented tangential to the e-beam [4]. For MWCNTs, displacement threshold energies correspond to 100 keV[4]. Once C atoms are displaced, lattice defect formation in the form of interstitials and vacancies will take place. Based on quantum mechanics calculations, defects on the form of di-vacancies, interstitials and Frenkel pair (interstitial-vacancy pair) defects, were shown to crosslink graphitic layers [23]. However, at the same time e-beam irradiation can lead to unwanted loss of lattice coherence, a process known as amorphitization. This is related to the kinetics of defects (production rate, dynamics) on specific sites of the C lattice and agglomeration of point defects that leads to larger defects. The dynamics of defects depend on temperature. E-beam irradiation at room temperature (as in this work) leads to the formation of vacancies and interstitials (for energies above the threshold energy), however both remain relatively localized (immobile) at specific lattice sites, and if they do not recombine to form cross-linking sites, it can lead to a high concentration and agglomeration of defects as e-beam time increases, which eventually causes the lattice to lose its crystallinity at those sites. This model is consistent with the amorphous regions encountered in Figures 5c-5e.

In terms of electrical results, our data can be explained in terms of a competitive process between crosslinking and amorphitization. Crosslinking sites reduce the resistivity by reducing the CNT to CNT distance, while amorphitization increases resistivity. Note that the reduction of resistivity by crosslinking events is not due to the conduction of electrons through sp^3 C-C bonds. The increase in resistivity at 10 min of e-beam irradiation can be explained by the formation of defects in the lattice that have not produced enough cross-linking sites that enhance conductivity. At irradiation times of 20-30 minutes, although crosslinking events are increasing, the resistivity is dominated by amorphitization events. The reduction of resistivity at 60 min can only be explained by a significant increase in crosslinking population that dominates the overall electrical conduction of electrons in the yarn. This is consistent with the microstructural data presented in Figure 5.

Conclusion

In summary, this is the first report on the e-beam irradiation effects on the electrical resistivity of CNT yarns. The author conducted systematic e-beam irradiation experiments on a TEM, follow by two probe analysis in an SEM. Both crosslinking and amorphous regions within the CNT yarn were observed by HRTEM, and both appear to increase with irradiation. Resistivity data were explained taking into account microstructural changes. The resistivity lower bound value corresponds to the maximum dosage used, and was below the resistivity of the pristine yarn. Taking into consideration (from other reports) that e-beam induced crosslinking can improve the mechanical properties of the yarn; our data suggests that e-beam processing can be a suitable route to achieve multifunctional CNT yarns. Note that we expect more significant improvement in regard to mechanical improvements of CNT yarns using the e-beam protocol of the current study. As pointed out by Cornwell and Welch (using molecular dynamics simulations), short fibers with just few cross-link density number can considerably improve fiber strength [24]. In contrast to the results presented by Mikó et al., CNTs within the yarn structure of the current study do not completely transform to a-C during irradiation.

Although it was established that 200 keV energies can induce cross-linked MWCNTs within the yarn, aspects about crosslinking uniformity across the entire cross section of the yarn needs further investigation. This is more critical in regards to the mechanical properties, because regions that are weaker due to less crosslinking densities can potentially start to fail faster than areas with high crosslinking densities, and those relative weak sites may further grow in size causing failure of the

yarn at lower strength values than expected. Note that the penetration of electrons at 200 keV (~234 μm for carbon material) is enough to penetrate the whole CNT yarn, however, the corresponding mean free path of electrons is just below 1.5μm [25]. This means that the electrons will suffer energy loss beyond a depth of ~1.5 μm. How much and how dependent is on depth is unknown at the moment, but if the energy loss is below the threshold energy displacement of C atoms, crosslinking will not take place.

Acknowledgement

This work was supported by the NASA Space Technology MissionDirectorate's Game Changing-Carbon Nanotube Materials Development Project.

References

1. Filleter T, Espinosa HD (2013) Multi-scale mechanical improvement produced in carbon nanotube fibers by irradiation cross-linking. Carbon 56: 1-11.
2. Kis A, Csányi G, Salvetat JP, Lee TN, Couteau E, et al. (2004) Reinforcement of single-walled carbon nanotube bundles by intertube bridging. Nat Mater 3: 153-157.
3. Xia ZH, Guduru P, Curtin WA (2007) Enhancing mechanical properties of multi-wall carbon nanotubes via sp^3 interwall bridging. Phys Rev Lett 98: 245501.
4. Krasheninnikov AV, Nordlund K (2010) Ion and electron irradiation-induced effects in nanostructured materials. J Appl Phys 107: 071301.
5. Peng B, Locascio M, Zapol P, Li S, Mielke SL, et al. (2008) Measurements of near-ultimate strength for multiwalled carbon nanotubes and irradiation-induced crosslinking improvements. Nat Nanotechnol 3: 626-631.
6. Filleter T, Bernal R, Li S, Espinosa HD (2011) Ultrahigh strength and stiffness in cross-linked hierarchical carbon nanotube bundles. Adv Mater 23: 2855-2860.
7. Lebrón-Colón M, Meador MA, Gaier JR, Solá F, Scheiman DA, et al. (2010) Reinforced thermoplastic polyimide with dispersed functionalized single wall carbon nanotubes. ACS Appl Mater Interfaces 2: 669-676.
8. Mikó C, Milas M, Seo JW, Couteau E, Barišić N, et al. (2003) Effect of electron irradiation on the electrical properties of fibers of aligned single-walled carbon nanotubes. Appl Phys Lett 83: 4622-4624.
9. Mikó C, Seo JW, Gaál R, Kulik A, Forró L (2006) Effect of electron and ultraviolet irradiation on aligned carbon nanotube fibers. Phys Status Solidi b 243: 3351-3354.
10. Solá F, Xia Z, Lebrón-Colón M, Meador MA (2012) Transmission electron microscopy of single wall carbon nanotube/polymer nanocomposites: A first-principles study. Phys Status Solidi RRL 6: 349-351.
11. Solá F, Niu J, Xia Z (2013) Heating induced microstructural changes in graphene/Cu nanocomposites. J Phys D: Appl Phys 46: 065309.
12. Steigerwald MDG, Arnold R, Bihr J, Drexel V, Jaksch H, et al. (2004) New detection system for GEMINI. Microsc Microanal 10: 1372.
13. Solá F, Hurwitz F, Yang J (2011) A new scanning electron microscopy approach to image aerogels at the nanoscale. Nanotechnology 22: 175704.
14. Solá F, Biaggi-Labiosa A, Fonseca LF, Resto O, Lebrón-Colón M, et al. (2009) Field Emission and Radial Distribution Function Studies of Fractal-like Amorphous Carbon Nanotips. Nanoscale Res Lett 4: 431-436.
15. Sears K, Skourtis C, Atkinson K, Finn N, Humphries (2010) Focused ion beam milling of carbon nanotube yarns to study the relationship between structure and strength. Carbon 48: 4450-4456.
16. Weeden O (2003) Probe card tutorial. Keithley Instruments, Inc., 24370303: 1-40.
17. Chen Q, Wang S, Peng LM (2006) Establishing Ohmic contacts for in situ current-voltage characteristic measurements on a carbon nanotube inside the scanning electron microscope. Nanotechnology 17: 1087-1098.
18. Rebouillat S, Lyons MEG (2011) Measuring the electrical conductivity of single fibres. Int J Electrochem Sci 6: 5731-5740.
19. Miao M (2011) Electrical conductivity of pure carbon nanotube yarns. Carbon 49: 3755-3761.
20. Miller SG, Williams TS, Baker JS, Solá F, Lebrón-Colón M, et al. Increased tensile strength of carbon nanotube yarns and sheets through chemical modification and electron beam irradiation, under review.
21. Lambin Ph, Loiseau A, Culot C, Biró LP (2002) Structure of carbon nanotubes probed by local and global probes. Carbon 40: 1635-1648.
22. Solá F, Lebrón-Colón M, Ferreira PJ, Fonseca LF, Meador MA, et al. (2010) In-situ TEM-STM observations of SWCNT ropes/tubular transformations. Mater Res Soc Symp Proc 1204: 1204-K10-26.
23. Telling RH, Ewels CP, El-Barbary AA, Heggie MI (2003) Wigner defects bridge the graphite gap. Nat Mater 2: 333-337.
24. Cornwell CF, Welch CR (2011) Very-high-strength (60-GPa) carbon nanotube fiber design based on molecular dynamics simulations. J Chem Phys 134: 204708.
25. Yao N, Wang ZL (2005) Handbook of microscopy for nanotechnology. 362-363 pages..